Ion Multivalence and Like-Charge Polyelectrolyte Attraction

John C. Butler,[1] Thomas Angelini,[1] Jay X. Tang,[2] and Gerard C. L. Wong[1,*]

[1]*Department of Materials Science & Engineering, Department of Physics, Department of Bioengineering, University of Illinois at Urbana-Champaign, Urbana, Illinois 61801, USA*

[2]*Department of Physics, Brown University, Providence, Rhode Island 02912, USA*

(Received 25 March 2003; published 11 July 2003)

It is known empirically that multivalent ions generate attractions between like-charged polyelectrolytes, with different valence requirements for different systems. How multivalent must an ion be before it can condense a given polyelectrolyte? Using charge-tunable *M*13 virus rods and a family of artificial homologous "dumbbell" divalent ions of different sizes, we have constructed a multivalent ion-polyelectrolyte phase diagram, and find an experimentally motivated general criterion for like-charged attraction based on the ion valence, ion size, and the Gouy-Chapman length.

DOI: 10.1103/PhysRevLett.91.028301 PACS numbers: 82.35.Rs, 82.35.Pq, 87.16.Ka

Electrostatics in aqueous media is fundamental to a broad range of phenomena in colloid science, soft condensed matter physics, and biology [1], such as chromosome organization, gene therapy, colloidal stabilization, and water treatment. According to mean field theories, such as the widely used Poisson-Boltzmann formalism, like-charged polyelectrolytes always repel [2]. Indeed, DNA chains in water containing monovalent ions repel one another. However, in the presence of *multivalent* ions, like-charge *attractions* [3–16] have been observed in a wide range of polyelectrolyte systems. Recent examples [17–20] include DNA, F-actin, microtubules, and filamentous viruses. Further, it is known that generally trivalent ions are required to condense DNA, while only divalent ions are required to condense F-actin and viruses of the Ff family. What makes a multivalent ion qualitatively different from a monovalent ion in this context? More generally, for a specific polyelectrolyte, what is the criterion that separates a multivalent ion capable of generating attractions from one that does not?

Polyelectrolytes in aqueous solution are coated by a condensed layer of mobile oppositely charged counterions. Theoretical models for like-charged polyelectrolyte attractions usually introduce correlations in this counterion layer. Dynamic correlated long wavelength "van der Waals"-like fluctuations in the counterion layer have been suggested as one possible mechanism [3–6]. Static counterion correlations along the axis of the polyelectrolyte rods in the form of a Wigner lattice have also been proposed [9–11,15]. Gronbech-Jensen *et al.* find that attractions exist regardless of the valence in the low temperature limit, and have proposed that the attraction-generating correlated fluctuations are washed out for monovalent ions [11]. Shklovskii *et al.* [9] have suggested that strongly interacting multivalent ions can form a correlated liquid on the polyelectrolyte surface, which generate image charges that lead to attractions, whereas weakly interacting monovalent ions cannot.

While these ideas are important for guiding our intuition, the current understanding remains incomplete: For example, what happens at the onset of polyelectrolyte attraction at low global multivalent ion concentrations, when the number of condensed ions may be small? Experimentally, ions with larger hydrated sizes tend to become less "multivalent," and in general larger threshold ion concentrations are needed before condensation [19]. Using natural divalent ions of different hydrated sizes (analogous to a Hofmeister series) does not give one enough variation to continuously tune the behavior from condensing to noncondensing regimes. Moreover, specific binding of a given ion can strongly modify condensation behavior: Divalent cations such as Mn^{2+} and Cd^{2+} preferentially adsorb onto the grooves of DNA and condense DNA, while Ca^{2+} or Mg^{2+} bind to the sugar-phosphate backbone of DNA, and do not [18].

In order to investigate the role of ion multivalence and geometry, we studied polyelectrolyte condensation using the anionic rodlike *M*13 virus, and a series of "tunable" divalent cations, $H_3N(CH_2)_nNH_3$, where $n = 1, 2, 3, 4$ [98.0% purity, Fluka ($n = 1$) and Aldrich ($n = 2-4$), Fig. 1(c)]. These diamine ions consist of two amine (+ 1) groups separated by n CH_2 groups [21]. Intuitively, a dumbbell ion consisting of two charges separated by a short spacer chain should behave as a multivalent ion and generate attractions. However, as the spacer chain length increases, the ion should eventually behave locally like two monovalent ions, and fail to generate attractions. The effective "multivalence" of the ions can therefore be continuously tuned, without changing the *p*H. (For example, histamine is monovalent at $pH = 7$ and divalent at $pH = 3$, but such large *p*H changes will affect the polyelectrolyte charge density drastically.) Since these ions have homologous structures with identical cationic charge groups, effects from differential specific binding are minimized. This approach also allows us to directly calculate the distances between the amine groups for each ion, so that estimate values for hydrated ion radii, which are unreliable and can change under different environmental conditions, need not be used. Surprisingly, we find that a small change in the ion size can lead to

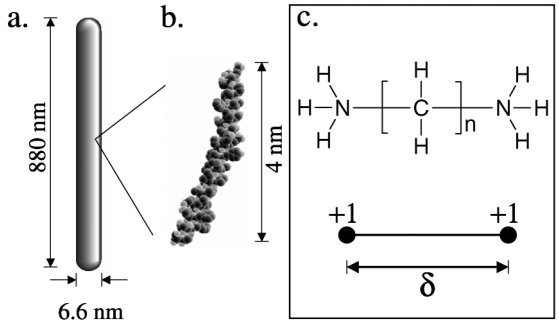

FIG. 1. Schematic representations of (a) the polyelectrolyte $M13$ virus, (b) the major coat protein on $M13$, which is repeated $\sim 2700\times$ on the viral surface, and (c) the tunable diamine ions (fully protonated). As the number of carbon atoms (n) in the spacer is increased, the spatial separation between the charged amine groups (δ) increases (e.g., for $n = 1$ and 2, $\delta = 0.29$ and 0.37 nm, respectively).

qualitatively different condensation behavior: The difference of a *single* CH_2 group in the spacer chain can drive the system from noncondensing to condensing behavior. Moreover, by adjusting the protonation state and therefore the surface charge density of the rodlike virus, we can control whether a given ion will condense the $M13$ virus. Based on this data, we propose a general structural criterion for attraction-inducing multivalent ions based on the ion size relative to the effective Gouy-Chapman length, and show that this proposed criterion is consistent with results on other polyelectrolyte systems.

The surface of each filamentous bacteriophage $M13$ virus is comprised of approximately 2700 copies of a major coat protein which package the single-stranded circular viral DNA into a rod (persistence length ~ 2 μm) with a total length of 880 nm and a diameter of 6.6 nm [Figs. 1(a) and 1(b)] [22]. This major coat protein is a charged α helix consisting of 50 residues, and constitutes the bulk of the total charge on the virus [23]. Because of its repetitive surface structure, $M13$ has a relatively smooth charge density compared to other biopolymers such as DNA and F-actin. Freeze-dried $M13$ and their host *Escherichia Coli* (strain K38) were purchased from the American Type Culture Collection (Manassas, VA). The progeny phages were separated from the bacteria media by multiple steps of sedimentation and resuspension, followed by a final separation step using the cesium-chloride density gradient method. The $M13$ virus rods are initially suspended in a pH 7.0 solution (5 mM Tris, 1 mM NaN_3). All x-ray samples have a final $M13$ virus concentration of 7.5 mg/ml, and have been sealed in quartz capillaries.

Small angle x-ray scattering (SAXS) measurements have been used to monitor the condensation behavior of the composite polyelectrolyte-ion system, using both an in-house x-ray source as well as beam line 4-2 at the Stanford Synchrotron Radiation Laboratory (SSRL). For the in-house experiments, incident CuKα radiation ($\lambda = 1.54$ Å) from a Rigaku rotating-anode generator is monochromatized and focused using Osmic confocal multilayer optics, and scattered radiation is collected on a Bruker 2D wire detector (pixel size = 105 μm). For the SSRL experiments, incident synchrotron x rays from the BL-4-2 8-pole Wiggler have been monochromatized using a double-bounce Si(111) crystal ($\lambda = 1.3806$ Å), and focused using a cylindrical mirror, and the scattered radiation has been collected using a MAR Research charged-coupled device camera (pixel size = 79 μm). The 2D SAXS data from both setups have been checked for mutual consistency.

In order to measure the divalent ion size required to condense the $M13$ virus at neutral pH, a series of SAXS experiments have been performed on virus samples with each of the diamines described above ($n = 1$ to 4). The global ion concentration in the $M13$ samples has been varied from 30 to 100 mM for each type of diamine ion, and the condensation behavior has been monitored using SAXS. The 2D SAXS patterns from these solution samples have been circularly averaged and plotted in Fig. 2. No condensation has been observed for the $n = 2$, 3, and 4 divalent diamines. SAXS data from these samples consist of smooth, featureless scattering expected from a solution of rods [$S(q)$ varies as $q^{-\alpha}$, where $\alpha = 1 \pm 0.1$]. As the length of the spacer is decreased to $n = 1$ (methylenediamine), a new correlation peak at 0.970 nm^{-1} becomes visible, which corresponds to $D = 6.48$ nm, consistent with the $M13$ diameter. As the size of the divalent ion decreases from 0.37 to 0.29 nm at neutral pH, it gains the ability to condense the $M13$ virus into close-packed aggregates.

Instead of changing the distance between charges on the diamine ion, we can also tune the distance in between the charges on the surface of the virus. The above experiment showed that it is possible to condense the $M13$ virus if the charge separation of the divalent ion is 0.29 nm. If we decrease the charge density of the virus and effectively increase the average spatial separation of charge on

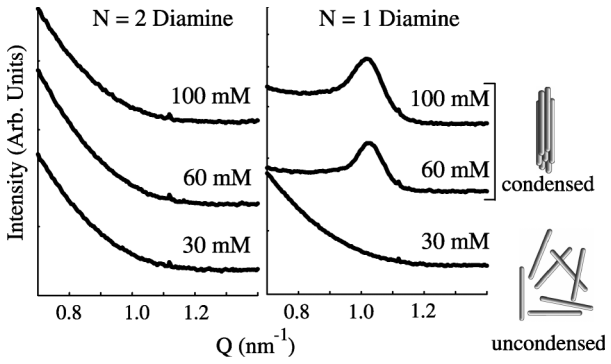

FIG. 2. Circularly averaged x-ray diffraction data of $M13$ for different diamine ion concentrations at neutral pH: No indication of $M13$ condensation is observed for the $N = 2$ diamine (same for the $N = 3$, 4 diamines). In the presence of the $N = 1$ diamine, however, bundling peaks corresponding to close-packed bundles are observed at 60 mM and above.

the surface of $M13$, can we decondense the $M13$ viruses which have been aggregated using the $n = 1$ diamine? The $M13$ virus has a well-defined surface charge density that can be controlled by changing the pH of the system. Approximately six of the 50 residues (and the amino terminus) are solution accessible and contribute to the surface charge on $M13$ [22]. By changing the pH, we change the protonation states of the amino acids on the virus' major coat protein, thereby modifying the surface charge density. If we assume that the solvent inaccessible residues do not contribute to the surface charge, then we can accurately calculate the surface charge of $M13$ using the Henderson-Hasselbach equation [24]. These charge calculations have been shown to agree quite well with experiment [25]. We estimate the pK of the $n = 1$ diamine to be at least 8.8, so that the ion is divalent in the pH range of interest. In order to avoid possible specific buffer influences to system behavior, as well as changes in the diamine ions themselves, we tune the pH over a small range using PIPES buffer only.

Changing the surface charge of the virus dramatically affects the ability of the diamines to condense the virus, as indicated by the data in Fig. 3. A wide range of $n = 1$ diamine data (40–140 mM) at pH range of 6.4 to 7.5 has been collected. Only 60 mM of the $n = 1$ diamine (methylenediamine) is sufficient to condense $M13$ at $p\mathrm{H} = 6.6$ ($M13$ surface charge density of $\sigma_{M13} = 0.303e^-/\mathrm{nm}^2$). As the pH is changed to 7.5 using the same PIPES buffer ($\sigma_{\mathrm{M13}} = 0.343e^-/\mathrm{nm}^2$) at the same diamine concentration, the system decondenses. In fact, condensation is not observed until the diamine concentration reaches 100 mM. In contrast, the $n = 2$ diamine does not condense $M13$ over the range of pH investigated. Figure 3(c) is a phase diagram which combines data for all the diamine types, concentrations (40–200 mM), and pH values studied, and shows the generic nonmonotonic salt dependence of condensation, with condensation followed by decondensation with increasing salt concentrations, as described by fluctuation theories, for example [26]. More importantly, the phase boundary which separates condensing and noncondensing behavior is clearly a function of the polyelectrolyte surface charge density.

The data in the phase diagram can be directly compared with theoretical approaches based on attraction-generating, strongly correlated liquids of multivalent ions [9,15], in which a Coulomb coupling constant $\Gamma = Z^2e^2/\epsilon RkT$ is defined to differentiate between different regimes of behavior (for multivalent ions of charge Ze in a medium of dielectric constant ϵ and temperature T, with R as the effective radius of ions on the surface of the polyelectrolyte.) If $\Gamma \simeq 1$, then mean field theory applies and like-charged rods repel. However, if $\Gamma \gg 1$, then a 2D strongly correlated liquid of classical charged particles is formed on the surfaces of the rods, and attractions are possible. For the diamine-$M13$ system, $\Gamma \sim 2$. Interestingly, when Γ is tuned over a narrow range, between 1.9 and 2.1, we find that the system evolves from noncondensing to condensing.

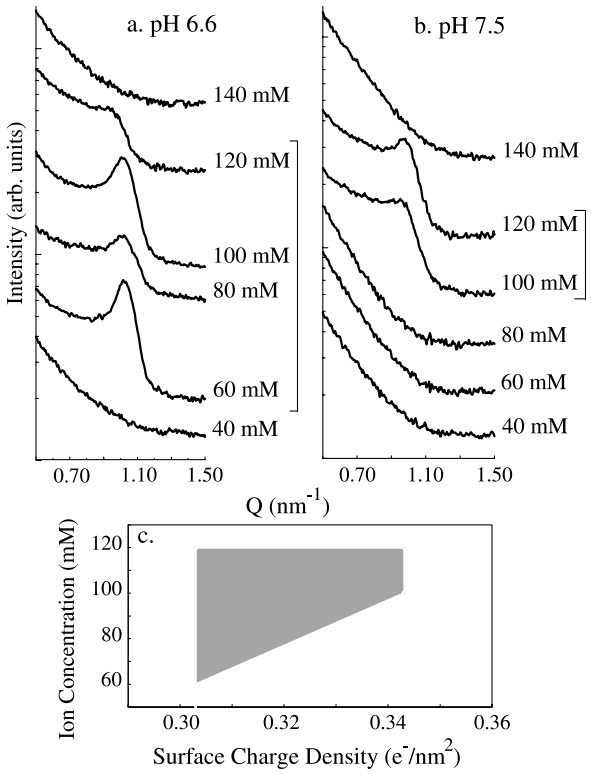

FIG. 3. X-ray diffraction data for the $N = 1$ diamine at (a) pH 6.6 and (b) pH 7.5. The circularly averaged scattering intensities for six different concentrations are shown for both surface charge environments. As the pH of the solution is raised (corresponding to an increase in the surface charge density of the virus), the virus needs a higher diamine concentration to condense (bracketed traces). (c) Phase diagram for polyelectrolyte condensation as a function of the polyelectrolyte charge density and the ion concentration.

What about the ion valence and size? If we examine the phase diagram on Fig. 3(c), we find that the charge separation on the diamines is typically several times smaller than the typical charge separation on the polyelectrolyte surface for *both* the condensing *and* noncondensing regimes, so that is not a crucial criterion. However, the minimum charge separation on the divalent ions is quite close to the Gouy-Chapman length defined with respect to the polyelectrolyte surface, which is analogous to a screening length in the present context. In our experiments, we have independently varied both λ and δ, where $\lambda = kT\epsilon/2\pi\sigma Ze$ is the Gouy-Chapman length (σ is the surface charge density), and δ is the spatial charge separation on the divalent ion. If we define the dimensionless parameter $R = \lambda/\delta$, our results indicate that a value of $R > 1$ is generally required to condense the polyelectrolyte. Since the screening lengths are small in the present physical situation, the electrostatic interactions are extremely short ranged. Let us assume that the size of the divalent ion is smaller than the charge

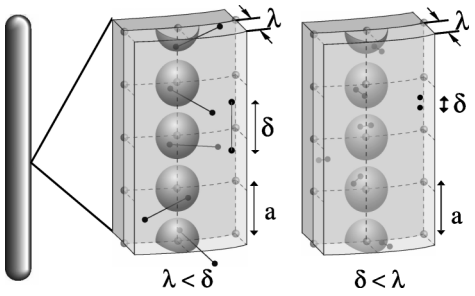

FIG. 4. A schematic of the polyelectrolyte surface: When $\delta > \lambda$, the adsorption of a divalent ion can only locally neutralize the surface at best. However, if $\delta < \lambda$, then a local charge inversion is possible upon adsorption, and a "sticky" patch is created on the polyelectrolyte rod, which can generate attractions (see text).

separation on the surface of the polyelectrolyte rod (which is the case here as well as in most physically important systems.) When $\delta > \lambda$ ($R < 1$), the adsorption of a divalent ion can only locally neutralize the surface at best. However, if $\delta < \lambda$ ($R > 1$), then a local charge inversion is possible upon adsorption, and a "sticky" patch is created on the polyelectrolyte rod, which can in turn bind to other polyelectrolyte rods, thus precipitating the onset of condensation (Fig. 4). Alternately, because the thickness of the condensed layer is $\sim\lambda$, a divalent ion that has an effective size $\delta > \lambda$ will be partially screened and behave effectively as a monovalent.

If we generalize this argument by approximating a natural divalent ion as a small assembly of point charges having a spatial extent defined by the size of its hydration shell (typically ~0.3 nm), we find that this model predicts condensation of F-actin ($R \sim 2.2$) and microtubules ($R \sim 1.9$) and noncondensation of DNA ($R \sim 0.5$) by divalent ions, in agreement with experiments [27]. We believe these results are important for the onset of attractions, where the density of condensed ions is small, before other ion correlation mechanisms take hold. However, we expect this simple argument to break down for rods of small radii (such as DNA), since the Gouy-Chapman length is strictly speaking only defined for a plane, and does not take into account ion size and associated excluded volume. For a complete understanding of these effects, a proper theoretical and computational treatment will be necessary.

We are grateful to R. Golestanian, P. Pincus, B. Shklovskii, and P. Braun for helpful discussions, and K. Ito and H. Tsuruta for their assistance at SSRL. This material is based upon work supported by NSF DMR-0071761, the NSF AMWP STC, Grant No. 00G0 from the Cystic Fibrosis Foundation, and the U.S. Department of Energy, Division of Materials Sciences under Grant No. DEF G02-91ER45439, through the Frederick Seitz Materials Research Laboratory at the University of Illinois at Urbana-Champaign.

*Corresponding author.
Electronic address: gclwong@uiuc.edu

[1] W. M. Gelbart, R. F. Bruinsma, P. A. Pincus, and V. A. Parsegian, Phys. Today **53**, No. 9, 38 (2000).
[2] J. Israelachvili, *Intermolecular and Surface Forces* (Academic, London, 1992), 2nd ed.
[3] J. G. Kirkwood and J. B. Shumaker, Proc. Natl. Acad. Sci. U.S.A. **38**, 863 (1952).
[4] F. Oosawa, *Polyelectrolytes* (Marcel Dekker, New York, 1971).
[5] B. Y. Ha and A. J. Liu, Phys. Rev. Lett. **79**, 1289 (1997).
[6] R. Podgornik and V. A. Parsegian, Phys. Rev. Lett. **80**, 1560 (1998).
[7] A. P. Lyubartsev, J. X. Tang, P. A. Janmey, and L. Nordenskiold, Phys. Rev. Lett. **81**, 5465 (1998).
[8] M. J. Stevens, Phys. Rev. Lett. **82**, 101 (1999).
[9] B. I. Shklovskii, Phys. Rev. Lett. **82**, 3268 (1999).
[10] A. A. Kornyshev and S. Leikin, Phys. Rev. Lett. **82**, 4138 (1999).
[11] N. Gronbech-Jensen, R. J. Mashl, R. F. Bruinsma, and W. M. Gelbart, Phys. Rev. Lett. **78**, 2477 (1997).
[12] G. S. Manning, Q. Rev. Biophys. **2**, 179 (1978).
[13] P. Pincus and S. A. Safran, Europhys. Lett. **42**, 103 (1998).
[14] R. Netz and H. Orland, Eur. Phys. J. E **1**, 203 (2000).
[15] I. Rouzina and V. A. Bloomfield, J. Phys. Chem. **100**, 9977 (1996).
[16] A. W. C. Lau, S. Safran, and P. Pincus, Phys. Rev. E **65**, 051502 (2002).
[17] V. A. Bloomfield, Biopolymers **31**, 1471 (1991).
[18] V. A. Bloomfield, Curr. Opin. Struct. Biol. **6**, 334 (1996).
[19] J. X. Tang and P. A. Janmey, J. Biol. Chem. **271**, 8556 (1996).
[20] R. Podgornik, D. Rau, and V. A. Parsegian, Biophys. J. **66**, 962 (1994).
[21] The diamines dissolve readily in water, and remain divalent for the *p*H ranges used in this investigation. Since the ions are highly charged, aggregation of the short hydrophobic spacer chains on the diamines is not thermodynamically favorable.
[22] L. A. Day, C. J. Marzec, S. A. Reisberg, and A. Casadevall, Ann. Rev. Biophys. Biophys. Chem. **17**, 509 (1988).
[23] L. Makowski and M. Russel, in *Structural Biology of Viruses*, edited by W. Chiu, R. M. Burnett, and R. L. Garcia (Oxford, New York, 1997).
[24] L. Strayer, *Biochemistry* (W. H. Freeman and Company, New York, 1995), 4th ed.
[25] K. Zimmermann, H. Hagedorn, C. C. Heuck, M. Hinrichsen, and H. Ludwig, J. Biol. Chem. **261**, 1653 (1986).
[26] R. Golestanian and T. B. Liverpool, Phys. Rev. E **66**, 051802 (2002).
[27] The difference in condensation behavior between *M*13 and *fd* can also be explained by geometry and the molecular details of the charge arrangement on the viruses. These results will be published in a forthcoming article.